

Ferrimagnetism in $\text{EuFe}_4\text{Sb}_{12}$ due to the Interplay of f -Electron Moments and a Nearly Ferromagnetic Host

V. V. Krishnamurthy,¹ J. C. Lang,² D. Haskel,² D. J. Keavney,² G. Srajer,² J. L. Robertson,¹ B. C. Sales,¹ D. G. Mandrus,¹ D. J. Singh,¹ and D. I. Bilc^{1,3}

¹Materials Science and Technology Division, Oak Ridge National Laboratory, Oak Ridge, Tennessee 37831, USA

²Advanced Photon Source, Argonne National Laboratory, Argonne, Illinois 60439, USA

³Department of Physics, University of Tennessee, Knoxville, Tennessee 37996, USA

(Received 17 May 2006; published 20 March 2007)

We combine x-ray magnetic circular dichroism spectroscopy at Fe $L_{2,3}$ edges, at Eu $M_{4,5}$ edges, x-ray absorption spectroscopy (XAS) investigation of Eu valence, and local spin density calculations, to show that the filled skutterudite $\text{Eu}_{0.95}\text{Fe}_4\text{Sb}_{12}$ is a ferrimagnet in which the Fe $3d$ moment and the Eu^{2+} $4f$ moment are magnetically ordered with dominant antiferromagnetic coupling. From Eu L_3 edge XAS, we find that about 13% of the Eu have a formal valence of $3+$. We ascribe the origin of ferrimagnetism at a relatively high transition temperature T_C of 85 K in $\text{Eu}_{0.95}\text{Fe}_4\text{Sb}_{12}$ to f -electron interaction with the nearly ferromagnetic $[\text{Fe}_4\text{Sb}_{12}]^{2-}$ host lattice.

DOI: 10.1103/PhysRevLett.98.126403

PACS numbers: 71.27.+a, 61.10.Ht, 75.30.Mb, 75.50.Bb

The filled skutterudites RM_4X_{12} (R = Rare earth, M = Fe, Ru, Os, aX = Sb, P) exhibit different electronic ground states such as superconductivity, ferromagnetic ordering, and heavy-fermion behavior [1–3]. Despite several experimental and theoretical efforts [1], the nature of the magnetic interaction between the rare earth and transition metal ions is not clear. Therefore, detailed studies of the element specific contributions to the total magnetization in ferromagnetic or nearly ferromagnetic skutterudites are important in order to gain a clear picture of the true magnetic ground state.

The observation of magnetic ordering in the filled skutterudite $\text{Eu}_{0.95}\text{Fe}_4\text{Sb}_{12}$ at the relatively high temperature of 85 K is unexpected [4]. If divalent Eu is replaced by divalent Ba, Sr, or Yb, no magnetic ordering occurs; while if iron is replaced by isovalent Ru, as in $\text{EuRu}_4\text{Sb}_{12}$, ferromagnetism is found only below 3 K [1]. The nonlinear temperature dependence of the reciprocal susceptibility χ^{-1} (see Fig. 1) suggests either a canted ferromagnetic or ferrimagnetic structure below the Curie temperature $T_C = 85$ K. Magnetization measurements (Fig. 1) on our polycrystalline specimens show that the net magnetic moment of the compound is about $5.1\mu_B/\text{f.u.}$ at 5 K, similar to that found in single crystals [5]. Both of these values are much less than the moment of $7\mu_B$ expected for a Eu^{2+} .

In this Letter, we report the element specific magnetism in $\text{Eu}_{0.95}\text{Fe}_4\text{Sb}_{12}$. To elucidate the origin of unusual magnetic properties of $\text{Eu}_{0.95}\text{Fe}_4\text{Sb}_{12}$, the robust nature of its magnetic ordering and the true ground state, we have investigated the valence state of Eu by measuring the x-ray absorption spectrum (XAS) at both the Eu $M_{4,5}$ ($3d$ to $4f$ transition) and $L_{2,3}$ ($2p$ to $5d$) edges. The element specific magnetic moments on Eu and Fe were probed using the Eu $M_{4,5}$ edge and Fe $L_{2,3}$ edge x-ray magnetic circular dichroism (XMCD) spectroscopy [6–8]. From these experiments, we find that each Eu^{2+} ion has a total

magnetic moment of $7.2 \pm 0.3\mu_B$ and 10%–15% of the Eu have a Eu^{3+} configuration. Each Fe has a small moment of $-0.21 \pm 0.03\mu_B$, resulting in a net moment of about $5\mu_B$ per formula unit (f.u.).

Polycrystalline samples of $\text{Eu}_y\text{Fe}_4\text{Sb}_{12}$ and a Eu^{2+} reference compound $\text{Eu}_8\text{Ga}_{16}\text{Ge}_{30}$ were prepared as de-

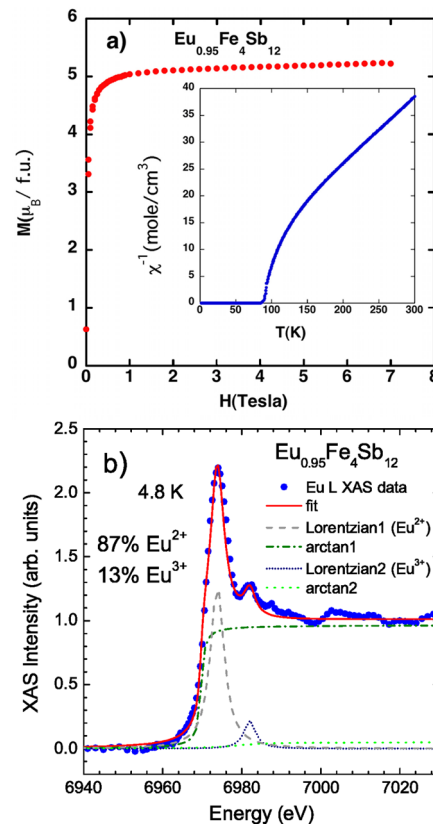


FIG. 1 (color online). (a) Magnetization vs field at 5 K in $\text{Eu}_{0.95}\text{Fe}_4\text{Sb}_{12}$. Inset shows χ^{-1} vs T . (b) Eu L_3 edge XAS with a fit described in the text.

scribed in Ref. [9] and were characterized by x-ray diffraction (XRD) and magnetization. The Eu site filling fraction y was estimated to be close to 0.95 from XRD intensity analysis. XAS measurements at the Eu $L_{2,3}$ edges were performed at the Advanced Photon Source (APS) beam line 4-ID-D. The x-ray absorption coefficient, which is defined as $\mu(E) = \frac{(\mu^+ + \mu^-)}{2}$, where μ^+ and μ^- are the x-ray absorption measured with positive and negative photon helicities, respectively, was measured at the Eu $L_{2,3}$ edges in $\text{Eu}_{0.95}\text{Fe}_4\text{Sb}_{12}$ and compared with that in the divalent europium reference compound $\text{Eu}_8\text{Ga}_{16}\text{Ge}_{30}$. Figure 1 shows Eu L_3 XAS of $\text{Eu}_{0.95}\text{Fe}_4\text{Sb}_{12}$. A strong peak from Eu^{2+} as in the XAS of $\text{Eu}_8\text{Ga}_{16}\text{Ge}_{30}$, and a satellite peak from Eu^{3+} are observed. The relative contributions of Eu^{2+} and Eu^{3+} were determined by fitting Eu L_3 edge XAS measured at 4.8 K and 295 K using a two-component model [10] that yielded a temperature independent population of 87% for Eu^{2+} and 13% for Eu^{3+} .

The XAS and XMCD measurements at the Eu $M_{4,5}$ and Fe $L_{2,3}$ edges were performed on beam line 4-ID-C using a hot pressed and highly polished pellet sample in an applied field of 2 Tesla. Figure 2 shows the XAS and XMCD at the Eu $M_{4,5}$ edges in $\text{Eu}_{0.95}\text{Fe}_4\text{Sb}_{12}$ measured at 4.9 K in an applied field of 2 Tesla. XMCD is defined as $\Delta\mu(E) = (\mu^+ - \mu^-)$. The XAS at the M_5 edge shows at least four peaks that could be associated with the multiplet splittings of Eu^{2+} and Eu^{3+} ions. The positions of the multiplet peaks in $M_{4,5}$ XAS compare quite well with the theoretical positions of Eu^{2+} and Eu^{3+} ions reported in the literature [11]. The M_4 edge XAS of $\text{Eu}_{0.95}\text{Fe}_4\text{Sb}_{12}$ was fit using linear combination of the relative contributions of the theoretical XAS of Eu^{2+} and Eu^{3+} . The best fit to the M_4 edge XAS, shown in Fig. 2(c), yielded $48 \pm 2\%$ of Eu^{2+} and $52 \pm 2\%$ of Eu^{3+} valence states. The contribu-

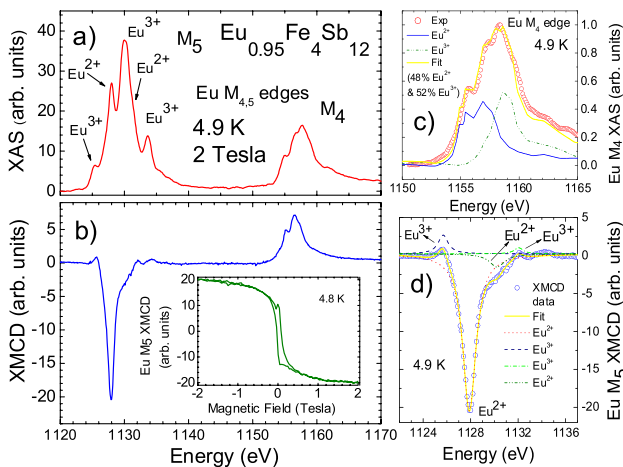


FIG. 2 (color online). Eu $M_{4,5}$ edge (a) XAS and (b) XMCD in $\text{Eu}_{0.95}\text{Fe}_4\text{Sb}_{12}$ measured in a field of 2 Tesla at 4.8 K. (c) Theoretical fit to Eu M_4 XAS. (d) Lorentzian fit to the M_5 edge XMCD data. Inset in (b) shows the hysteresis of M_5 edge XMCD peak intensity at $E = 1128$ eV at 4.8 K.

tion of Eu^{3+} , estimated from the soft XAS measurement at the M_4 edge, is much larger than the 13% found in the hard XAS measurement at the L_3 edge. We attribute the discrepancy to the different fractions in the mixed valence at the surface, since the soft x-ray measurements only probe the top 5 nm of the sample while the L -edge measurements are a bulk probe. However, we can use the obtained values of Eu^{2+} and Eu^{3+} occupancies to normalize our XMCD signal from Eu^{2+} . A fit by Lorentzians to the XMCD spectrum [see Fig. 2(d)] shows that about 92% of the integrated XMCD intensity belongs to Eu^{2+} and the remaining 8% originates from a Van-Vleck type contribution from the low lying excited states of Eu^{3+} . Because the XMCD measured at the Eu $M_{4,5}$ edges, shown in Fig. 2(b), is associated with a $4f$ final state, it directly gives a measure of the magnetic polarization in the $4f$ shell of Eu ions. The hysteresis [inset in Fig. 2(b)] shows that the Eu moment is saturated at 2 Tesla. The sum rule analysis enables the estimation of spin and orbital magnetic moments of Eu from the measured intensities of XAS and XMCD [12]. We assumed that the magnetic dipole operator, $\langle T_Z \rangle = 0$ which is reasonable as Eu has cubic symmetry and $L = 0$ for Eu^{2+} . The sum rule analysis of the experimental Eu $M_{4,5}$ edge XAS and the XMCD, shown in Fig. 2, the Eu^{2+} valence population of $48 \pm 2\%$, together with the assumptions of 7 unoccupied states in the $4f$ shell ($N_{4f} = 7$) has yielded $\mu_{\text{orb}} = 0.13 \pm 0.1 \mu_B$ and $\mu_{\text{spin}} = 7.07 \pm 0.3 \mu_B$ per Eu^{2+} ion. The total moment of Eu^{2+} is therefore $7.2 \pm 0.3 \mu_B$.

Figure 3 shows the Fe $L_{2,3}$ edge XAS and XMCD in $\text{Eu}_{0.95}\text{Fe}_4\text{Sb}_{12}$ measured at 2.3 K in the ferromagnetic state, in a field of 2 Tesla. The spectra at 130 K above T_C did not show any appreciable signal indicating that the surface of the skutterudite sample was free of magnetic impurities during the measurements. Double peak or multiple peaks

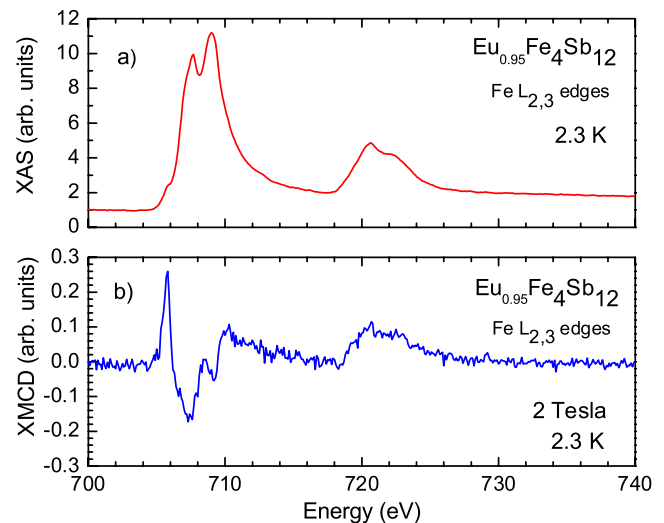


FIG. 3 (color online). Fe $L_{2,3}$ edge (a) XAS and (b) XMCD in $\text{Eu}_{0.95}\text{Fe}_4\text{Sb}_{12}$ showing that Fe is magnetically ordered.

in the XAS can occur either from two different valent states of Fe or the energy-level splitting of the $3d$ state of Fe for a single valence state due to a crystal field or a combination of these. The presence of an XMCD shows that Fe has an ordered magnetic moment in this compound. The observed XMCD line shape consists of peaks at about 705.5 eV and 710 eV and minima at 707.5 and 709 eV in the L_3 edge region. Considering that Fe has a single site in this compound, we can estimate the magnetic moment per Fe from the XMCD spectrum. Using the magneto-optic sum rules for the $L_{2,3}$ edges of $3d$ group metals [12], the spin and orbital contributions to the $3d$ magnetic moment of Fe in $\text{Eu}_{0.95}\text{Fe}_4\text{Sb}_{12}$ are determined from the observed intensities of XAS and XMCD. Following a procedure similar to that used by Chen *et al.* [13], with the number of $3d$ holes $N_{3d} = 3.4$ found in XAS, and assuming that $\langle T_Z \rangle = 0$, we get $-0.07 \pm 0.02\mu_B$ and $-0.14 \pm 0.02\mu_B$ for the orbital moment and the spin moment of Fe, respectively. The total Fe moment is then $-0.21 \pm 0.03\mu_B$. The sign of the Fe moment indicates that it is antiferromagnetically coupled to the Eu moment, which was shown to have a positive sign in the analysis presented earlier. The Fe moment value is comparable to the value of $0.25\mu_B/\text{Fe}$ atom reported from dc magnetization measurements in $\text{AFe}_4\text{Sb}_{12}$ ($A = \text{Na}, \text{K}$) [14] and is consistent with a small hyperfine splitting observed in the ^{57}Fe Mössbauer spectra in these compounds. The total magnetic moment due to Fe in the unit cell of $\text{Eu}_{0.95}\text{Fe}_4\text{Sb}_{12}$ is then $-0.84 \pm 0.12\mu_B$. If we consider the antiferromagnetic alignment of the net moment of Fe with the $7.2 \pm 0.3\mu_B$ per Eu^{2+} ions, and that the Eu^{2+} contribution of 87% obtained from the analysis of bulk sensitive Eu L_3 XAS, and the Eu site filling fraction of 0.95, then the total moment of $\text{Eu}_{0.95}\text{Fe}_4\text{Sb}_{12}$ comes out to be $5.1 \pm 0.3\mu_B$ per formula unit. This is in excellent agreement with the net moment of $\sim 5.1\mu_B/\text{f.u.}$ found in dc magnetization. While our results support the antiparallel alignment, we cannot fully rule out a canted structure or a more complex arrangement, due to the uncertainty in the magnitude of moments from our measurement.

The calculations were done within the local spin density approximation (LSDA) using the general potential LAPW method [15] and the crystal structure as determined experimentally at 100 K [5]. Converged results were obtained with a sampling of 48 points in the symmetry irreducible wedge of the zone. We employed basis sets of approximately 3100 basis functions including local orbitals [15], which were used to relax linearization errors and to include the upper semicore states. The core states were treated relativistically, while the valence states were treated in a scalar relativistic approximation. We find two magnetic states in fixed spin moment calculations, both with fully occupied majority spin Eu f bands and fully unoccupied minority spin f bands (i.e., Eu^{2+}). The lower energy state is the predicted ground state and is borderline half-metallic with a spin magnetization of $5.02\mu_B/\text{f.u.}$ consisting of

$7\mu_B/\text{Eu}$ and $-0.5\mu_B/\text{Fe}$. The other state, which is 0.128 eV/Eu higher in energy, has a spin magnetization of $8.26\mu_B/\text{f.u.}$. Both states have the same polarization inside the Eu atom centered spheres to within $0.01\mu_B$, corresponding to $7\mu_B$ from the Eu f and an induced polarization of $0.38\mu_B/\text{f.u.}$ (from 12 Sb atoms) mainly from Sb p derived states, which extend into the Eu atom centered sphere (radius $2.3a_0$). The magnitude of polarization in the Sb p states may, however, be exaggerated in the LSDA, similar to the case in Ce filled skutterudites [16]. In fact, we found no observable dichroism signal at the Sb $M_{4,5}$ edges in our XMCD experiments. We also performed self-consistent density functional calculations including spin-orbit interaction and found an average Fe orbital moment of $-0.06\mu_B$ that is parallel to the Fe spin moment. The calculations with spin-orbit interaction yielded the same ground state with practically the same spin moments as the scalar relativistic calculations. Thus the magnetism should be described as arising from an antiferromagnetic coupling of the $7\mu_B$ Eu f moment with a host magnetization consisting of a $\sim 2\mu_B$ Fe spin moment and a $\sim 0.2\mu_B$ Fe orbital moment, both on a per formula unit basis. This is distinct from an induced magnetization due to hybridization with Eu because in that case there would be no metastable state with the host magnetization parallel to the Eu magnetization. The orbital moment of Fe agrees with the value from Fe $L_{2,3}$ edge XMCD measurements, whereas the Fe spin moment is larger in the calculation. LSDA was found to overestimate the size of the ordered Fe spin moment by about $0.3\mu_B$ in related compounds $\text{AFe}_4\text{Sb}_{12}$ ($A = \text{Na}$ or K) [14]. A similar situation may be happening in our calculations. Alternatively, the smaller Fe spin moment observed in the XMCD experiment in a field of 2 Tesla could be due to a more complex spin arrangement in the Fe sublattice which reduces the net ferromagnetic component. Considering that the other $n_v = 23.5$ compounds, $\text{CaFe}_4\text{Sb}_{12}$, $\text{SrFe}_4\text{Sb}_{12}$, and $\text{BaFe}_4\text{Sb}_{12}$ are all highly renormalized paramagnets with evidence for ferromagnetic quantum fluctuations regardless of the different filling ion sizes [17], one may speculate that $\text{EuFe}_4\text{Sb}_{12}$ is an analogous compound, but that the quantum fluctuations are suppressed by interaction with the Eu. The ordering of Fe moments in $\text{EuFe}_4\text{Sb}_{12}$ found in our XMCD experiments indicates the absence of spin fluctuations, which prevent magnetic ordering of Fe in $\text{CaFe}_4\text{Sb}_{12}$. Spin fluctuations in Ca^{2+} and Ba^{2+} filled iron antimonides are shown to be suppressed by a magnetic field [14].

The electronic density of states (DOS) for the anti-aligned ground state is shown in Fig. 4. As may be seen, the Fe derived DOS is exchange split by ~ 0.5 eV, opposite to the Eu splitting. The majority spin Fe valence bands are completely occupied (these are the down spin relative to the total magnetization). There is a small DOS extending upwards from the main valence band due to the light band characteristic of skutterudite antimonides, [18] but the

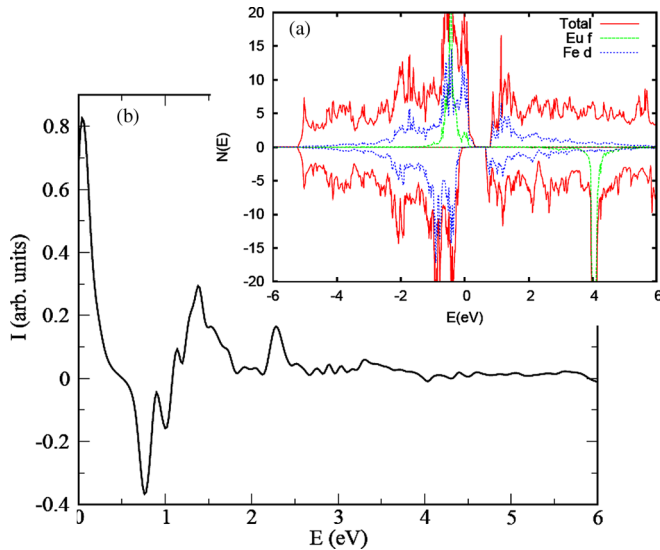


FIG. 4 (color online). (a) Electronic density of states and projections onto the sphere of Fe d and Eu f character, for magnetic $\text{EuFe}_4\text{Sb}_{12}$ on a per formula unit basis. Note that the narrow Eu f peaks are cut off by the scale. Majority spin is shown above the axis, and minority below. E_F is at 0 eV. (b) Calculated difference of Fe $2p$ XAS into spin up and spin down components with a 0.1 eV broadening.

main Fe d DOS does not reach the Fermi energy, E_F . On the other hand, there is a large up spin minority Fe d contribution to the DOS around E_F . In both spin channels, there is a gap followed by mixed character conduction bands which are also exchange split. At low energies the excitations will necessarily be to the spin up minority spin d states, since there are no spin down valence states below the energy of the conduction bands. As energy is increased, the valence band edge will be reached, and then the spin down conduction band edge. This will result in a change of sign followed by a long tail with another sign change. This is seen in Fig. 4 which shows the calculated difference of Fe x-ray absorption in the spin up and spin down channels. The correspondence with the experimental spectra of Fig. 2(b) supports the picture of a compound with Eu^{2+} moments interacting with a magnetic host lattice with the Fe moment opposite to the moment of Eu. This provides an example of a local moment f electron system interacting with a weak itinerant ferromagnetic host.

$\text{EuFe}_4\text{Sb}_{12}$ is found to be almost half-metallic, which is consistent with the point-contact Andreev reflection measurements by Sheet *et al.* on $\text{KFe}_4\text{Sb}_{12}$ [19]. The exchange interaction between the $3d$ electrons of Fe and the $4f$ electrons of Eu^{2+} suppresses the spin fluctuations of Fe in $\text{Eu}_{0.95}\text{Fe}_4\text{Sb}_{12}$ and helps to satisfy the Stoner criteria for

ferromagnetism, $I_{\text{ex}}N_f(E_F) \geq 1$, where I_{ex} is the effective exchange interaction and $N(E_F)$ is the density of states at E_F . Therefore, we conclude that the interaction of Eu $4f$ moments with the nearly ferromagnetic $[\text{Fe}_4\text{Sb}_{12}]^{2-}$ host lattice plays a key role in the stability of ferrimagnetism with an enhanced T_C in $\text{Eu}_{0.95}\text{Fe}_4\text{Sb}_{12}$.

Research sponsored by Materials Science and Engineering Division, Experimental User Facilities Division, Office of Basic Energy Sciences, US DOE under Contract No. DE-AC05-00OR22725 with ORNL, managed by UT-Battelle, LLC, and Office of Naval Research. The work at the APS, ANL is sponsored by the Office of Sciences, US DOE under Contract No. W-31-109-ENG-38.

- [1] B. C. Sales, in *Hand Book on the Physics and Chemistry of Rare Earths*, edited by K. A. Gschneidner, Jr., J.-C. G. Buzenli, and V.K. Pecharsky (Elsevier Science, Amsterdam, 2003), Vol. 33, pp. 1–34.
- [2] M. B. Maple *et al.*, *Physica (Amsterdam)* **259–261B**, 8 (1999).
- [3] V. Keppens *et al.*, *Nature (London)* **395**, 876 (1998).
- [4] E. Bauer *et al.*, *Phys. Rev. B* **63**, 224414 (2001).
- [5] E. D. Bauer *et al.*, *J. Phys. Condens. Matter* **16**, 5095 (2004).
- [6] A. P. Holm *et al.*, *J. Am. Chem. Soc.* **124**, 9894 (2002).
- [7] J. B. Kortright *et al.*, *J. Magn. Magn. Mater.* **207**, 7 (1999).
- [8] G. van der Laan *et al.*, *Phys. Rev. B* **34**, 6529 (1986).
- [9] B. C. Sales *et al.*, *Phys. Rev. B* **56**, 15081 (1997).
- [10] C. Godart *et al.*, *J. Less-Common Met.* **94**, 177 (1983).
- [11] B. T. Thole *et al.*, *Phys. Rev. B* **32**, 5107 (1985).
- [12] B. T. Thole, P. Carra, F. Sette, and G. van der Laan, *Phys. Rev. Lett.* **68**, 1943 (1992); P. Carra, B. T. Thole, M. Altarelli, and Xindong Wang, *Phys. Rev. Lett.* **70**, 694 (1993).
- [13] C. T. Chen *et al.*, *Phys. Rev. Lett.* **75**, 152 (1995).
- [14] A. Leithe-Jasper *et al.*, *Phys. Rev. Lett.* **91**, 037208 (2003); *Phys. Rev. B* **70**, 214418 (2004).
- [15] D. J. Singh and L. Nordstrom, *Plane Waves Pseudopotentials and the LAPW Method* (Springer, New York, 2006), 2nd ed. An in-house code for most calculations and the WIEN2K code for the x-ray absorption were used and were cross-checked; P. Blaha *et al.*, *WIEN2K, An Augmented Plane Wave + Local Orbitals Program for Calculating Crystal Properties* (Technische Universitaet Wien, Vienna, 2002).
- [16] L. Nordstrom and D. J. Singh, *Phys. Rev. B* **53**, 1103 (1996).
- [17] E. Matsuoka *et al.*, *J. Phys. Soc. Jpn.* **74**, 1382 (2005).
- [18] D. J. Singh and W. E. Pickett, *Phys. Rev. B* **50**, 11235 (1994); D. J. Singh and I. I. Mazin, *Phys. Rev. B* **56**, R1650 (1997).
- [19] G. Sheet *et al.*, *Phys. Rev. B* **72**, 180407(R) (2005).